Journal of Vibration Engineering & Technologies (2024) 12:971–978
https://doi.org/10.1007/s42417-023-00887-8

ORIGINAL PAPER

Positioning and Swing Elimination Control of the Overhead Crane System with Double-Pendulum Dynamics

Yijiang Zhao[1] · Xianqing Wu[1] · Fang Li[1] · Yibo Zhang[1]

Received: 7 December 2022 / Revised: 20 January 2023 / Accepted: 30 January 2023 / Published online: 13 February 2023
© Krishtel eMaging Solutions Private Limited 2023

Abstract

Purpose: For most existing control approaches, the overhead crane systems are usually modeled as the single-pendulum model. However, when the hook mass is too large to be ignored and the distance between the payload and the hook cannot be neglected, the crane exhibits double-pendulum dynamics. Therefore, the double-pendulum dynamics of the overhead crane systems are taken into consideration in this study.

Methods: A new enhanced anti-swing control strategy is developed for the positioning and swing elimination control of overhead crane systems. First, based on the system dynamic equations, an auxiliary control input is introduced. Then, an elaborate Lyapunov function is constructed and a nonlinear anti-swing control approach is presented for the overhead crane system with double-pendulum dynamics. Finally, rigorous theoretical analysis is given to prove the convergence of the system states, that is, positioning and swing elimination control objective is achieved.

Results and Conclusion: Simulation tests are included to verify the effectiveness and robustness of the devised approach. In addition, a comparison study between the proposed method and existing control methods is provided. The obtained simulation results show that the proposed control method possesses superior control performance.

Keywords Mechanical system · Vibration elimination · Overhead crane · Motion control · Underactuated system

Introduction

Underactuated mechanical systems, which have fewer actuators than degrees of freedom, are extensively applied in various industrial fields in recent years [1–11]. The overhead crane system, as a typical mechanical underactuated system, has been widely used in railway transportation, iron and steel chemical industry, port and other places, the main work of which is driving the payload smoothly and safely to its destination. Similar to other underactuated mechanical systems, the fact that the payload can be only indirectly controlled by the motion of the trolley brings a great challenge for the control of the overhead crane system.

Recently, a lot of control strategies have been presented for overhead crane systems. Specially, to suppress the swing of the payload, some energy-based approaches are developed for overhead crane systems [12–14]. In fact, the parameters of mechanical systems cannot be accurately known and the mechanical systems usually suffer from external disturbances. For the purpose of addressing the above mentioned issues, the adaptive control technology [15–17] and the sliding mode control technology [18, 19] are applied to the control of overhead crane systems. Moreover, some open-loop control strategies, including input shaping methods [20–22] and some methods based on trajectory planning [23, 24], are also developed to realize the control objectives for overhead cranes. Besides the traditional nonlinear approaches, some intelligent control algorithms are also presented to address the control problems of overhead crane systems in recent years [25–28].

It is worthwhile to point out that above-mentioned approaches model the overhead crane system as the single-pendulum model with the assumption that the payload and

✉ Xianqing Wu
wxq@zstu.edu.cn

Yijiang Zhao
yijiangz1996@163.com

Fang Li
liliya_99@163.com

Yibo Zhang
zhangy41@163.com

[1] School of Information Science and Engineering, Zhejiang Sci-Tech University, Hangzhou 310018, China

the hook are regarded as one mass point. For this assumption, the hook mass and the distance between the payload and hook are ignored. However, in practical overhead crane systems, the payload is usually connected to a hook through the steel cable, which means that there is a certain distance between the hook and the payload. In addition, the hook mass connected to the trolley is usually large, which cannot be neglected. Therefore, the hook and the payload will exhibit different swings and the single-pendulum assumption does not hold when the mass of the hook is too large and the distance between the payload and hook is not negligible. Therefore, the overhead crane systems behave double-pendulum dynamics (as shown in Fig. 1), which greatly increases the complexity of the dynamic model for the overhead crane system and even makes the methods presented for single-pendulum cranes invalid. To this end, some results have been reported in [29–33] to address the control issue of double-pendulum overhead crane systems. Especially, for the double-pendulum overhead cranes, Ref. [31] propose a new quasi-proportional integral derivative control method. For the purpose of improving the performance index, some optimal control approaches are also applied to double-pendulum cranes in [34–36].

For double-pendulum overhead cranes, the fact that three degrees of freedom need to be controlled by one control input makes the control problem for the overhead crane systems extremely challenging. Although some excellent and constructive works have been reported in the literature, some issues need to be solved. In particular, the interconnection and damping assignment passivity-based control (IDA-PBC) technique is used to the control of underactuated systems, where control methods are designed by solving a series of partial differential equations [14]. The passivity-based control is usually used to construct a suitable Lyapunov function for the double-pendulum overhead cranes, however, the energy damping rate only depends on the trolley [37]. To enhance the coupling behavior among the trolley movement, the hook swing, and the payload swing, a novel energy-coupling-based control method is introduced in [38], where the system dynamic model of the overhead crane needs to be linearized when making control design and stability analysis. With the motivation to address these problems, a new enhanced anti-swing control law is developed with the consideration of double-pendulum dynamics. More precisely, firstly, we implement some basic transformations on the system dynamics and the acceleration variable is regarded as the auxiliary control input to be designed. Next, both an elaborate Lyapunov function and a corresponding auxiliary control input are introduced. Subsequently, the final control strategy is developed for the double-pendulum overhead crane system. After that, the stability of the closed-loop system and the convergence of the system states are strictly analyzed using Lyapunov theory and LaSalle's invariance theorem. At last, the developed method is tested in Matlab/Simulink to demonstrate its effectiveness and robustness.

The rest sections of this paper are outlined as follows. In Sect. 2, the dynamic model of the overhead crane system is provided. In Sect. 3, controller design and corresponding stability analysis are given. Simulation tests are included in Sect. 4. Finally, some conclusions are made in Sect. 5.

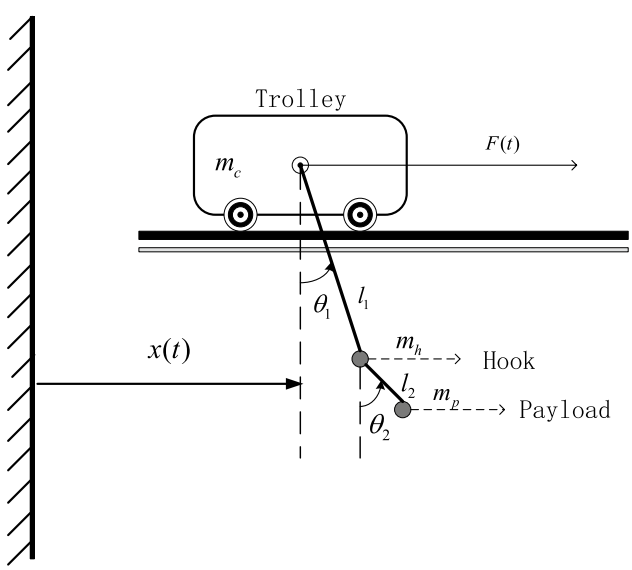

Fig. 1 Structure of the double-pendulum overhead crane system

Dynamic Model of the Overhead Crane System

In this paper, we consider the double-pendulum overhead crane system as shown in Fig. 1. By employing the Euler–Lagrange approach, the double-pendulum overhead crane system can be described with the following dynamics [31]

$$m_1\ddot{x} + m_2\ddot{\theta}_1\cos\theta_1 - m_2\dot{\theta}_1^2\sin\theta_1 + m_3\ddot{\theta}_2\cos\theta_2 - m_3\dot{\theta}_2^2\sin\theta_2 = F \tag{1}$$

$$m_2\ddot{x}\cos\theta_1 + m_2 l_1\ddot{\theta}_1 + m_4\ddot{\theta}_2\cos(\theta_1-\theta_2) + m_4\dot{\theta}_2^2\sin(\theta_1-\theta_2) + m_2 g\sin\theta_1 = 0 \tag{2}$$

$$m_3\ddot{x}\cos\theta_2 + m_4\ddot{\theta}_1\cos(\theta_1-\theta_2) + m_3 l_2\ddot{\theta}_2 - m_4\dot{\theta}_1^2\sin(\theta_1-\theta_2) + m_3 g\sin\theta_2 = 0 \tag{3}$$

where $x(t)$, $\theta_1(t)$, $\theta_2(t)$ represent the trolley displacement, hook swing angle and payload swing angle, respectively; the acceleration constant of the gravity is expressed by g;

the driving force is represented by $F(t)$; m_1, m_2, m_3, m_4 are system parameters, the explicit expressions of which are described as follows

$$m_1 = (m_c + m_h + m_p), m_2 = (m_h + m_p)l_1$$
$$m_3 = m_p l_2, m_4 = m_p l_1 l_2$$

where m_c, m_h, m_p represent the mass of the trolley, hook and payload, respectively; l_1 is the length of the rope; l_2 denotes the distance between the hook center and the payload center.

In this paper, the following auxiliary variables are introduced for the simplicity of the subsequent analysis process

$$S_1 = \sin\theta_1,\ \ S_2 = \sin\theta_2,\ \ S_{12} = \sin(\theta_1 - \theta_2)$$
$$C_1 = \cos\theta_1,\ C_2 = \cos\theta_2,\ C_{12} = \cos(\theta_1 - \theta_2)$$

Then, the equations of the dynamic (1)-(3) can be rewritten into a compact form as follows

$$M_{11}\ddot{x} + M_{12}\ddot{\theta} + V_1 = F \tag{4}$$

$$M_{21}\ddot{x} + M_{22}\ddot{\theta} + V_2 = 0 \tag{5}$$

where

$$\theta = [\theta_1\ \ \theta_2]^{\mathrm{T}},\ M_{11} = m_1$$
$$M_{12} = M_{21}^{\mathrm{T}} = [m_2 C_1\ \ m_3 C_2],\ V_1 = -m_2\dot{\theta}_1^2 S_1 - m_3\dot{\theta}_2^2 S_2$$
$$M_{22} = \begin{bmatrix} m_2 l_1 & m_4 C_{12} \\ m_4 C_{12} & m_2 l_2 \end{bmatrix},\ V_2 = \begin{bmatrix} m_2 g S_1 + m_4\dot{\theta}_2^2 S_{12} \\ m_3 g S_2 - m_4\dot{\theta}_1^2 S_{12} \end{bmatrix}$$

The main objectives of the double-pendulum overhead crane are driving the payload smoothly and safely to its destination and ensuring no residual swing of the payload and hook. To realize the objectives of the system, we will design a nonlinear control strategy to position the trolley to the specified location and suppress the swing of the hook and payload, which means

$$\lim_{t\to\infty}\left[x\ \ \theta_1\ \ \theta_2\ \ \dot{x}\ \ \dot{\theta}_1\ \ \dot{\theta}_2\right]^{\mathrm{T}} = \left[x_d\ \ 0\ \ 0\ \ 0\ \ 0\ \ 0\right]^{\mathrm{T}} \tag{6}$$

where $x_d \in \mathbb{R}$ is the specified location of the trolley.

For practical cranes, the following assumption is reasonably made [29, 31].

Assumption 1 The swing of the hook and payload is within $-\frac{\pi}{2} \le \theta_1, \theta_2 \le \frac{\pi}{2}$.

Main Results

In this section, a nonlinear control strategy will be developed to realize the control objectives of the double-pendulum overhead crane system. Moreover, rigorous stability analysis of the closed-loop system will be given to demonstrate the feasibility of the presented control method.

Controller Design

First, a partial feedback linearizing control law is derived as follows based on (4) and (5)

$$F = (M_{11} - M_{12}M_{22}^{-1}M_{21})\upsilon + V_1 - M_{12}M_{22}^{-1}V_2 \tag{7}$$

where $v(t) = \ddot{x}(t)$ is an auxiliary signal which should be designed. Thus, we could design a suitable acceleration signal $\ddot{x}(t)$ to obtain the desired controller.

For the double-pendulum overhead crane system, the total mechanical energy of which is

$$\begin{aligned} E_{\mathrm{hp}} = &\ \frac{1}{2}m_2 l_1\dot{\theta}_1^2 + \frac{1}{2}m_3 l_2\dot{\theta}_2^2 + m_4\dot{\theta}_1\dot{\theta}_2 C_{12} \\ &+ m_2 g(1 - C_1) + m_3 g(1 - C_2) \end{aligned} \tag{8}$$

Then, the derivative of $E_{hp}(t)$ can be obtained as follows

$$\begin{aligned} \dot{E}_{\mathrm{hp}} = &\ m_2 l_1\dot{\theta}_1\ddot{\theta}_1 + m_3 l_2\dot{\theta}_2\ddot{\theta}_2 + m_4\ddot{\theta}_1\dot{\theta}_2 C_{12} \\ &+ m_4\dot{\theta}_1\ddot{\theta}_2 C_{12} - m_4\dot{\theta}_1^2\dot{\theta}_2 S_{12} + m_4\dot{\theta}_1\dot{\theta}_2^2 S_{12} \\ &+ m_2 g\dot{\theta}_1 S_1 + m_3 g\dot{\theta}_2 S_2 \end{aligned} \tag{9}$$

Meanwhile, inserting (2) and (3) into $\dot{E}_{hp}(t)$ leads to

$$\dot{E}_{\mathrm{hp}} = -(m_2\dot{\theta}_1 C_1 + m_3\dot{\theta}_2 C_2)\cdot\upsilon \tag{10}$$

Based on $v(t)$ and $\dot{E}_{hp}(t)$, the following Lyapunov function candidate is introduced

$$V(t) = \frac{1}{2}k_p(e_x - k_v m_2 S_1 - k_v m_3 S_2)^2 + \frac{1}{2}\dot{x}^2 + k_v E_{\mathrm{hp}} \tag{11}$$

where $k_p, k_v \in \mathbb{R}^+$ are constants and $e_x(t)$ is the positioning error, that is

$$e_x = x - x_d \tag{12}$$

Next, taking the derivative of $V(t)$ along the closed-loop system (1)-(3) and making some algebraic manipulations yields

$$\begin{aligned} \dot{V}(t) = &\ (\dot{x} - k_v m_2\dot{\theta}_1 C_1 - k_v m_3\dot{\theta}_2 C_2)(\upsilon \\ &+ k_p(e_x - k_v m_2 S_1 - k_v m_3 S_2)) \end{aligned} \tag{13}$$

wherein the conclusion of (10) is used.

Based on (13), the following auxiliary input signal is designed

$$\begin{aligned} \upsilon = &-k_p(e_x - k_v m_2 S_1 - k_v m_3 S_2) - k_d(\dot{x} \\ &- k_v m_2\dot{\theta}_1 C_1 - k_v m_3\dot{\theta}_2 C_2) \end{aligned} \tag{14}$$

where $k_d \in \mathbb{R}^+$ is a constant. By inserting the above control scheme (14) into (7), one can get the controller as follows

$$F = (M_{11} - M_{12}M_{22}^{-1}M_{21})(-k_p(e_x - k_v m_2 S_1 - k_v m_3 S_2) - k_d(\dot{x} - k_v m_2 \dot{\theta}_1 C_1 - k_v m_3 \dot{\theta}_2 C_2)) + V_1 - M_{12}M_{22}^{-1}V_2 \tag{15}$$

Stability Analysis

In this section, to prove the stability of the closed-loop system and the convergence of the states, the following theorem is introduced.

Theorem 1 *The developed nonlinear control method ensures the control objectives of the double-pendulum overhead crane system are achieved, that is*

$$\lim_{t\to\infty} \left[e_x \;\; \theta_1 \;\; \theta_2 \;\; \dot{x} \;\; \dot{\theta}_1 \;\; \dot{\theta}_2\right]^{\mathrm{T}} = [0 \;\; 0 \;\; 0 \;\; 0 \;\; 0 \;\; 0]^{\mathrm{T}} \tag{16}$$

Proof First, the following Lyapunov function candidate given in (11) is introduced

$$V(t) = \frac{1}{2}k_p\left(e_x - k_v m_2 S_1 - k_v m_3 S_2\right)^2 + \frac{1}{2}\dot{x}^2 + k_v E_{\mathrm{hp}}$$

Taking the time derivative of $V(t)$, applying the conclusion of (10), and substituting the devised control law (15) into the resulting equation lead to

$$\dot{V}(t) = -k_d\left(\dot{x} - k_v m_2 \dot{\theta}_1 C_1 - k_v m_3 \dot{\theta}_2 C_2\right)^2 \le 0 \tag{17}$$

which means that $V(t) \in \mathcal{L}_\infty$ and the closed-loop system is stable in the Lyapunov sense. Furthermore, the following conclusion can be derived

$$x, \dot{x}, \theta_1, \dot{\theta}_1, \theta_2, \dot{\theta}_2 \in \mathcal{L}_\infty \tag{18}$$

To demonstrate that the origin is the only equilibrium point, the following invariant set is introduced based on LaSalle's invariance principle

$$\mathcal{S} = \left\{(x, \dot{x}, \theta_1, \dot{\theta}_1, \theta_2, \dot{\theta}_2) \mid \dot{V}(t) = 0\right\} \tag{19}$$

According to (19), one can obtain the following conclusion

$$\dot{x} - k_v m_2 \dot{\theta}_1 C_1 - k_v m_3 \dot{\theta}_2 C_2 = 0 \tag{20}$$

it is clear from (20) that

$$e_x - k_v m_2 S_1 - k_v m_3 S_2 = \alpha_1 \tag{21}$$

where $\alpha_1 \in \mathbb{R}$ is a constant. Thus, one can derive from (14), (20) and (21) that

$$\ddot{x} = \upsilon = -k_p(e_x - k_v m_2 S_1 - k_v m_3 S_2) = -k_p \alpha_1 \tag{22}$$

Then, we assume that $\upsilon(t) \neq 0$ and it can be concluded that

$$\dot{x}(t) \to \begin{cases} -\infty & \upsilon(t) < 0, \\ +\infty & \upsilon(t) > 0, \end{cases} \quad \text{as} \quad t \to \infty \tag{23}$$

The conclusion of (23) means that $x(t)$ will go infinity when t goes infinity, which contradicts the result of (18). Therefore, the supposition of $\upsilon(t) \neq 0$ is invalid, which further makes the following equality hold

$$\ddot{x} = \upsilon = -k_p(e_x - k_v m_2 S_1 - k_v m_3 S_2) = 0 \tag{24}$$

Analogously, one can get the following conclusion from (24)

$$\left.\begin{aligned} \dot{x} &= \alpha_2 \\ e_x &= k_v m_2 S_1 + k_v m_3 S_2 \end{aligned}\right\} \Longrightarrow \dot{x} = 0 \tag{25}$$

where $\alpha_2 \in \mathbb{R}$ is a constant. It is derived from (25) that

$$m_2 S_1 + m_3 S_2 = \alpha_3 \Longrightarrow m_2 \dot{\theta}_1 C_1 + m_3 \dot{\theta}_2 C_2 = 0 \tag{26}$$

where $\alpha_3 \in \mathbb{R}$ is a constant. To guarantee $\alpha_3 = 0$, the sum of (2) and (3) is written as

$$\frac{\mathrm{d}}{\mathrm{d}t}\left[m_2 l_1 \dot{\theta}_1 + m_3 l_2 \dot{\theta}_2 + m_4(\dot{\theta}_1 + \dot{\theta}_2)C_{12}\right] = -m_2 g S_1 - m_3 g S_2 \tag{27}$$

Integrating both sides of (27) yields

$$m_2 l_1 \dot{\theta}_1 + m_3 l_2 \dot{\theta}_2 + m_4(\dot{\theta}_1 + \dot{\theta}_2)C_{12} = -\alpha_3 g t + \alpha_4 \tag{28}$$

where $\alpha_4 \in \mathbb{R}$ is a constant. It can be derived that $\alpha_3 = 0$ from the conclusion of (18). Therefore, the following equalities hold

$$m_2 S_1 + m_3 S_2 = 0 \tag{29}$$

$$m_2 l_1 \dot{\theta}_1 + m_3 l_2 \dot{\theta}_2 + m_4(\dot{\theta}_1 + \dot{\theta}_2)C_{12} = \alpha_4 \tag{30}$$

According to the triangular transformation formula, one can rewrite the item $(\dot{\theta}_1 + \dot{\theta}_2)C_{12}$ of (30) as follows

$$\begin{aligned} (\dot{\theta}_1 + \dot{\theta}_2)C_{12} &= (\dot{\theta}_1 + \dot{\theta}_2)(C_1 C_2 + S_1 S_2) \\ &= (\dot{\theta}_1 C_1 C_2 + \dot{\theta}_2 S_1 S_2) + (\dot{\theta}_1 S_1 S_2 + \dot{\theta}_2 C_1 C_2) \end{aligned} \tag{31}$$

which further implies from (26) and (30) that

$$\begin{aligned} (\dot{\theta}_1 + \dot{\theta}_2)C_{12} &= -\frac{m_3}{m_2}(\dot{\theta}_2 C_2^2 + \dot{\theta}_2 S_2^2) - \frac{m_2}{m_3}(\dot{\theta}_1 S_1^2 + \dot{\theta}_1 C_1^2) \\ &= -\frac{m_3}{m_2}\dot{\theta}_2 - \frac{m_2}{m_3}\dot{\theta}_1 \end{aligned} \tag{32}$$

Substituting the resulting expression of (32) into (30) for $(\dot{\theta}_1 + \dot{\theta}_2)C_{12}$ and utilizing the expressions of m_2, m_3, m_4 lead to

$$
\begin{aligned}
&m_2 l_1 \dot{\theta}_1 + m_3 l_2 \dot{\theta}_2 + m_4(\dot{\theta}_1 + \dot{\theta}_2)C_{12} \\
&\quad = m_2 l_1 \dot{\theta}_1 + m_3 l_2 \dot{\theta}_2 - m_4\left(\frac{m_3}{m_2}\dot{\theta}_2 + \frac{m_2}{m_3}\dot{\theta}_1\right) \\
&\quad = \left(m_3 l_2 - \frac{m_4 m_3}{m_2}\right)\dot{\theta}_2 = \alpha_4
\end{aligned} \tag{33}
$$

Analogously, it is clear that

$$\alpha_4 = 0,\ \dot{\theta}_2 = 0 \tag{34}$$

which, along with (29) and (30), further indicates that

$$\dot{\theta}_1 = 0 \tag{35}$$

Based on (2), (3) and the conclusions that

$$\ddot{x} = 0,\ \dot{\theta}_1 = 0,\ \dot{\theta}_2 = 0,\ \ddot{\theta}_1 = 0,\ \ddot{\theta}_2 = 0 \tag{36}$$

Then, based on Assumption 1, one can obtain that

$$S_1 = 0,\ S_2 = 0 \Longrightarrow \theta_1 = 0,\ \theta_2 = 0 \tag{37}$$

By summarizing the results in (37), (21), (22) and (24), we can draw the conclusion that

$$e_x = 0 \Longrightarrow x = x_d \tag{38}$$

Hence, the conclusion of the theorem is proven.

Simulation Results

In this section, a series of digital simulation tests are included using Matlab/Simulink to demonstrate the control performance of the developed control law. Specially, three groups of simulation tests will be carried out. For the first group, the LQR method and an existing nonlinear control method designed in [31] are selected for a comparison study. For the second group, the control performance of the proposed method with different system parameters and desired positions will be examined. For the third group, the robustness of the proposed method with respect to different external disturbances will be examined.

Comparative Simulation

First, we set the initial condition as $[x(0)\ \theta_1(0)\ \theta_2(0)]^{\mathrm{T}} = [0\ 0\ 0]^{\mathrm{T}}$. The parameters of the system are adopted as

$$l_1 = 0.8\,\mathrm{m}, l_2 = 0.2\,\mathrm{m},\ m_c = 10\,\mathrm{kg},$$
$$m_h = 0.2\,\mathrm{kg}, m_p = 3\,\mathrm{kg}, g = 9.8\,\mathrm{kg/s^2}$$

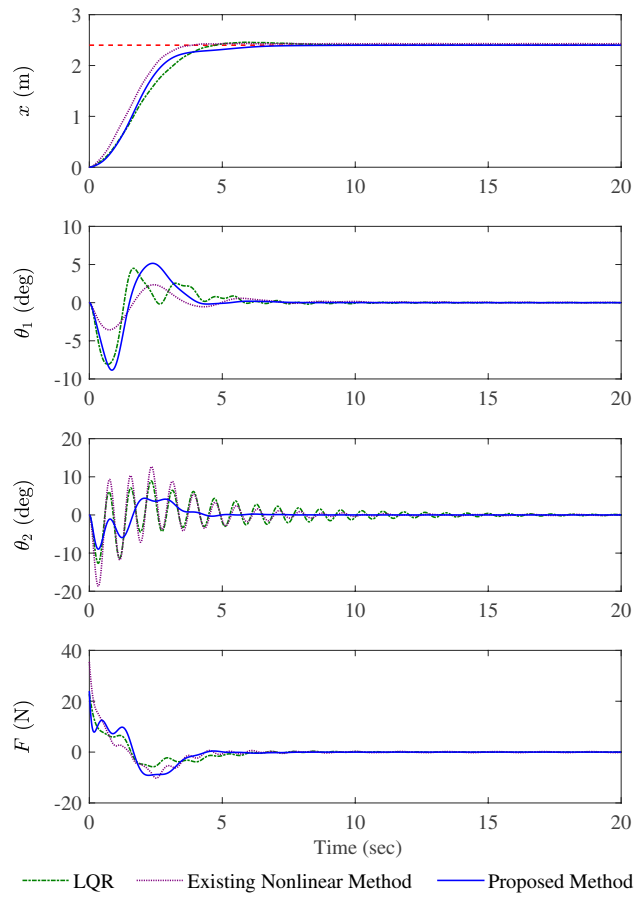

Fig. 2 Simulation results for the LQR method, the existing nonlinear method, and the presented approach

and the desired position is set as $x_d = 2.4\,\mathrm{m}$. The control gains of the presented approach are adopted as

$$k_p = 1,\ k_d = 2,\ k_v = 0.6$$

For simplicity, the expressions of the LQR method and the existing nonlinear control method are not given here. The simulation results of the three methods are displayed in Fig. 2.

It can be observed from Fig. 2 that the LQR method, the existing nonlinear control method and the developed method can make the trolley reach the specified position rapidly. However, we can also observe the fact that both the LQR method and the existing nonlinear control method need more time to eliminate the hook swing and even can not eliminate the payload swing, which affects work efficiency and sometimes causes payload damages in some cases. The comparative simulation results of this group show that the proposed control method possesses superior control performance.

Stabilization of Different Conditions

For the second simulation test, we will evaluate the control performance of the developed control law with different conditions. Specially, we will examine the performance of the devised control law with the following cases.

Case 1 The desired position is changed from $x_d = 2.4\,\mathrm{m}$ to $x_d = 1.8\,\mathrm{m}$. The initial condition is zero. The system parameters and control gains are selected as the same as those in the comparative simulation part.

Case 2 The system parameters are changed to $m_c = 7\,\mathrm{kg}$, $m_h = 0.1\,\mathrm{kg}$, $m_p = 1\,\mathrm{kg}$, $l_1 = 0.4\,\mathrm{m}$, $l_2 = 0.1\,\mathrm{m}$, $g = 9.8\,\mathrm{kg/s^2}$. The initial condition is zero. The desired position and control gains are chosen as the same as those in the comparative simulation part.

The simulation results of this group are displayed in Figs. 3 and 4, respectively. We can observe from Figs. 3 and 4 that the swing of the hook and payload is successfully suppressed and eliminated with different conditions. The simulation results show that the proposed method has good performance regardless of whether the desired position or system parameters are changed.

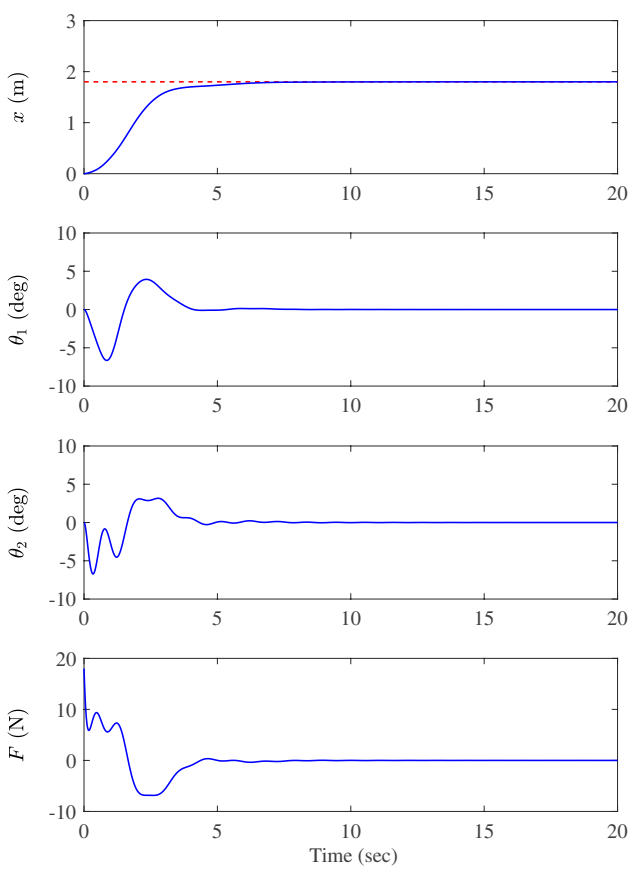

Fig. 3 Simulation results for the presented approach (15) with respect to Case 1

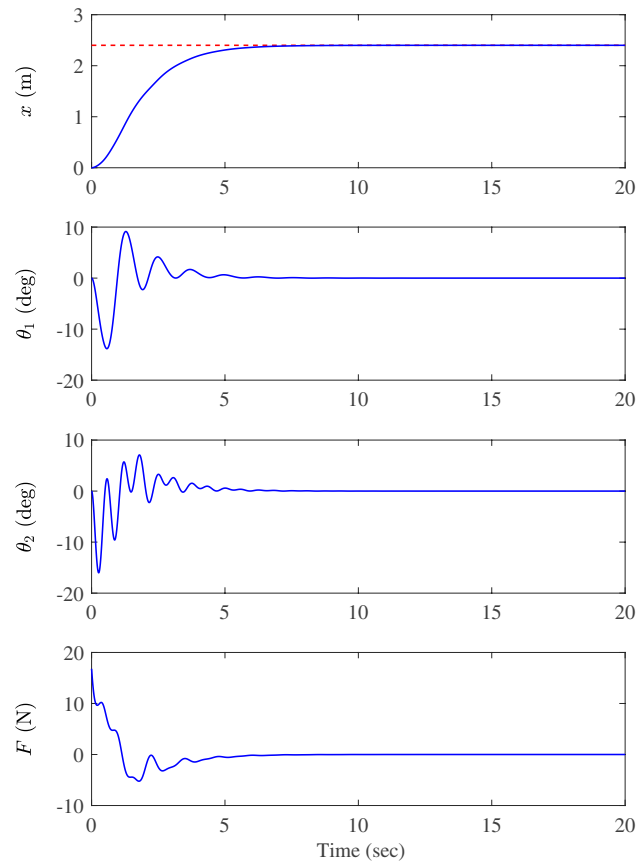

Fig. 4 Simulation results for the presented approach (15) with respect to Case 2

Robustness Examination

To examine the robustness of the proposed control method with respect to different external disturbances, we add three kinds of disturbances to the payload. Specifically, random disturbances are imposed on the payload between 10 and 15 s, sinusoid disturbances are imposed on the payload between 22 and 24 s, and impulsive disturbances are imposed on the payload between 30 and 30.1 s, all with the amplitude of 2°. All of other conditions are chosen as the same as those in the comparative simulation part.

The simulation results of this group are shown in Fig. 5. From the obtained simulation results, one can find that three

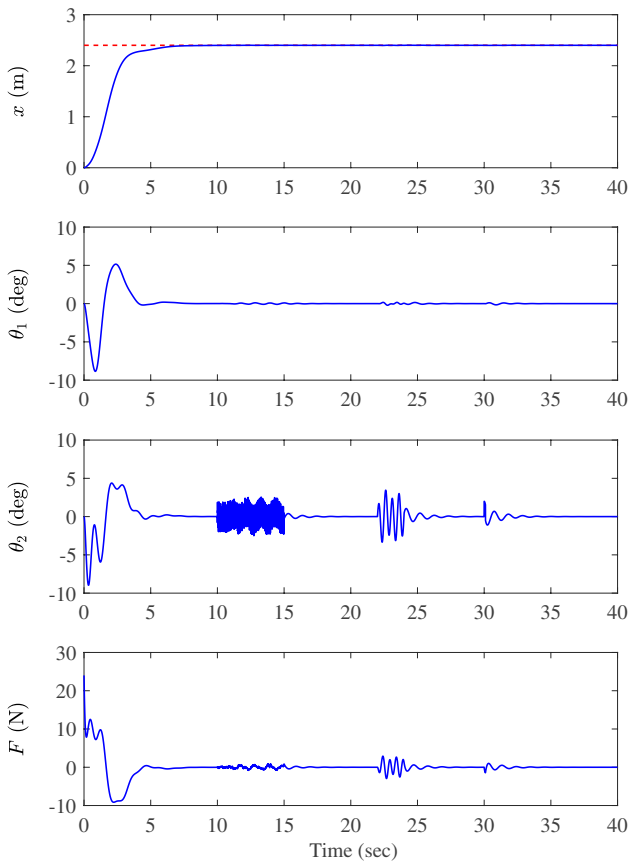

Fig. 5 Simulation results for the presented approach (15) with respect to different disturbances

types of external disturbances are all eliminated by the proposed control method, which indicates satisfactory robustness with respect to uncertain disturbances.

Conclusions

In this study, a new enhanced anti-swing control strategy is developed for overhead crane systems with double-pendulum dynamics. The presented control algorithm has both the theoretical and practical significance. On the one hand, the double pendulum-dynamics of the overhead crane system is taken into consideration to improve the applicability in practical engineering. On the other hand, a novel control strategy is presented to suppress the payload swing and hook swing. Compared with existing approaches for the double-pendulum overhead crane control, digital simulation results have shown that the presented approach has excellent performance.

Funding This work was supported by the Natural Science Foundation of Zhejiang Province (LY22F030014) and the National Natural Science Foundation of China (61803339).

Declarations

conflicts of interest The author(s) declared no potential conflicts of interest with respect to the research, authorship, and/or publication of this article.

References

1. Xu X, Zhang X, Zhu W, Gu X (2021) Modal parameter identification of a quayside container crane based on data-driven stochastic subspace identification. Journal of Vibration Engineering & Technologies 9(5):919–938
2. Lin J, Lai HY, Chang J (2018) Stabilization and equilibrium control for electrically cart-seesaw systems by neuro-fuzzy approach. Journal of Vibration Engineering & Technologies 6(1):1–11
3. Bettega J, Richiedei D, Tamellin I, Trevisani A. Model inversion for precise path and trajectory tracking in an underactuated, non-minimum phase, spatial overhead crane. Journal of Vibration Engineering & Technologies DOI: https://doi.org/10.1007/s42417-022-00786-4
4. Liu D, Lai X, Wang Y, Wan X, Wu M (2019) Position control for planar four-link underactuated manipulator with a passive third joint. ISA Trans 87:46–54
5. Chen H, Sun N (2020) Nonlinear control of underactuated systems subject to both actuated and unactuated state constraints with experimental verification. IEEE Trans Industr Electron 67(9):7702–7714
6. Li H, Wu Y, Chen M (2021) Adaptive fault-tolerant tracking control for discrete-time multiagent systems via reinforcement learning algorithm. IEEE Transactions on Cybernetics 51(3):1163–1174
7. Liang X, Zhang Z, Yu H, Wang Y, Fang Y, Han J (2022) Antiswing control for aerial transportation of the suspended cargo by dual quadrotor UAVs. IEEE/ASME Trans Mechatron 27(6):5159–5172
8. Liang X, Yu H, Zhang Z, Liu H, Fang Y, Han J (2023) Unmanned aerial transportation system with flexible connection between the quadrotor and the payload: Modeling, controller design and experimental validation. IEEE Trans Industr Electron 70(2):1870–1882
9. Sun N, Fang Y, Chen H, Wu Y, Lu B (2018) Nonlinear antiswing control of offshore cranes with unknown parameters and persistent ship-induced perturbations: Theoretical design and hardware experiments. IEEE Trans Industr Electron 65(3):2629–2641
10. Wu X, Zhao Y, Xu K (2021) Nonlinear disturbance observer based sliding mode control for a benchmark system with uncertain disturbances. ISA Trans 110:63–70
11. Xing L, Wen C, Liu Z, Su H, Cai J (2017) Event-triggered adaptive control for a class of uncertain nonlinear systems. IEEE Trans Autom Control 62(4):2071–2076
12. Sun N, Fang Y, Zhang X (2013) Energy coupling output feedback control of 4-DOF underactuated cranes with saturated inputs. Automatica 49(5):1318–1325
13. Wu X, He X (2015) Enhanced damping-based anti-swing control method for underactuated overhead cranes. IET Control Theory Appl 9(12):1893–1900

14. Wu X, He X (2017) Nonlinear energy-based regulation control of three-dimensional overhead cranes. IEEE Trans Autom Sci Eng 14(2):1297–1308
15. Sun N, Fang Y, Chen H, He B (2015) Adaptive nonlinear crane control with load hoisting/lowering and unknown parameters: Design and experiments. IEEE/ASME Trans Mechatron 20(5):2107–2119
16. Lu B, Fang Y, Sun N (2020) Adaptive output-feedback control for dual overhead crane system with enhanced anti-swing performance. IEEE Trans Control Syst Technol 28(6):2235–2248
17. Zhao B, Ouyang H, Iwasaki M (2022) Motion trajectory tracking and sway reduction for double-pendulum overhead cranes using improved adaptive control without velocity feedback. IEEE/ASME Trans Mechatron 27(5):3648–3659
18. Chwa D (2017) Sliding-mode-control-based robust finite-time antisway tracking control of 3-D overhead cranes. IEEE Trans Industr Electron 64(8):6775–6784
19. Wu X, Xu K, Lei M, He X (2020) Disturbance-compensation-based continuous sliding mode control for overhead cranes with disturbances. IEEE Trans Autom Sci Eng 17(4):2182–2189
20. Jaafar HI, Mohamed Z, Shamsudin MA, Mohd Subha NA, Ramli L, Abdullahi AM (2019) Model reference command shaping for vibration control of multimode flexible systems with application to a double-pendulum overhead crane. Mech Syst Signal Process 115:677–695
21. Maghsoudi MJ, Mohamed Z, Sudin S, Buyamin S, Jaafar HI, Ahmad SM (2017) An improved input shaping design for an efficient sway control of a nonlinear 3D overhead crane with friction. Mech Syst Signal Process 92:364–378
22. Maghsoudi MJ, Ramli L, Sudin S, Mohamed Z, Husain AR, Wahid H (2019) Improved unity magnitude input shaping scheme for sway control of an underactuated 3D overhead crane with hoisting. Nonlinear Dyn 123:466–482
23. Chen H, Fang Y, Sun N (2016) Optimal trajectory planning and tracking control method for overhead cranes. IET Control Theory Appl 10(6):692–699
24. Zhang X, Fang Y, Sun N (2014) Minimum-time trajectory planning for underactuated overhead crane systems with state and control constraints. IEEE Trans Industr Electron 61(12):6915–6925
25. Le HX, Van Nguyen T, Le AV, Phan TA, Nguyen NH, Phan MX (2019) Adaptive hierarchical sliding mode control using neural network for uncertain 2D overhead crane. International Journal of Dynamics and Control 7(3):996–1004
26. Ramli L, Mohamed Z, Jaafar HI (2018) A neural network-based input shaping for swing suppression of an overhead crane under payload hoisting and mass variations. Mech Syst Signal Process 107:484–501
27. Rong B, Rui X, Tao L, Wang G (2018) Dynamics analysis and fuzzy anti-swing control design of overhead crane system based on Riccati discrete time transfer matrix method. Multibody Sys-Dyn 43(3):279–295
28. Yu W, Li X, Panuncio F (2014) Stable neural PID anti-swing control for an overhead crane. Intelligent Automation and Soft Computing 20(2):145–158
29. Lu B, Fang Y, Sun N (2019) Enhanced-coupling adaptive control for double-pendulum overhead cranes with payload hoisting and lowering. Automatica 101:241–251
30. Li M, Chen H, Zhang R (2022) An input dead zones considered adaptive fuzzy control approach for double pendulum cranes with variable rope lengths. IEEE/ASME Trans Mechatron 27(5):3385–3396
31. Sun N, Yang T, Fang Y, Wu Y, Chen H (2019) Transportation control of double-pendulum cranes with a nonlinear quasi-PID scheme: Design and experiments. IEEE Transactions on Systems, Man, and Cybernetics: Systems 49(7):1408–1418
32. Zhang M, Ma X, Chai H, Rong X, Tian X, Li Y (2016) A novel online motion planning method for double-pendulum overhead cranes. Nonlinear Dyn 85(2):1079–1090
33. Zhang M, Ma X, Rong X, Tian X, Li Y (2016) Adaptive tracking control for double-pendulum overhead cranes subject to tracking error limitation, parametric uncertainties and external disturbances. Mech Syst Signal Process 76–77:15–32
34. Chen H, Fang Y, Sun N (2017) A swing constrained time-optimal trajectory planning strategy for double pendulum crane systems. Nonlinear Dyn 89(2):1513–1524
35. Wu Q, Wang X, Hua L, Xia M (2020) Dynamic analysis and time optimal anti-swing control of double pendulum bridge crane with distributed mass beams. Mech Syst Signal Process 144:106968
36. Wu Q, Wang X, Hua L, Xia M (2021) Improved time optimal anti-swing control system based on low-pass filter for double pendulum crane system with distributed mass beam. Mech Syst Signal Process 151:107444
37. Sun N, Wu Y, Fang Y, Chen H (2018) Nonlinear antiswing control for crane systems with double-pendulum swing effects and uncertain parameters: Design and experiments. IEEE Trans Autom Sci Eng 15(3):1413–1422
38. Zhang M, Ma X, Rong X, Song R, Tian X, Li Y (2018) (2018) A novel energy-couplingbased control method for double-pendulum overhead cranes with initial control force constraint. Adv Mech Eng 10(1):1–13

Publisher's Note Springer Nature remains neutral with regard to jurisdictional claims in published maps and institutional affiliations.

Springer Nature or its licensor (e.g. a society or other partner) holds exclusive rights to this article under a publishing agreement with the author(s) or other rightsholder(s); author self-archiving of the accepted manuscript version of this article is solely governed by the terms of such publishing agreement and applicable law.